Dynamic tissue analysis using time- and wavelength-resolved fluorescence spectroscopy for atherosclerosis diagnosis

Yinghua Sun,[1,2] Yang Sun,[1] Douglas Stephens,[1] Hongtao Xie,[1] Jennifer Phipps,[1] Ramez Saroufeem,[3] Jeffrey Southard,[4] Daniel S. Elson,[5] and Laura Marcu[1,2]

[1]Department of Biomedical Engineering, University of California, Davis, 451 Health Sciences Drives, Davis, California 95616, USA
[2]NSF Center for Biophotonics Science and Technology, University of California, Davis, 2700 Stockton Blvd, Sacramento, California 95817, USA
[3]Department of Medical Pathology and Laboratory Medicine, 4400 V Street, Sacramento, California 95817, USA
[4]Division of Cardiovascular Medicine, UC Davis Medical Center, 4860 Y Street, Sacramento, California 95817, USA
[5]Institute of Biomedical Engineering, Imperial College London, Exhibition Road, London, SW7 2AZ, UK
**lmarcu@ucdavis.edu*

Abstract: Simultaneous time- and wavelength-resolved fluorescence spectroscopy (STWRFS) was developed and tested for the dynamic characterization of atherosclerotic tissue *ex vivo* and arterial vessels *in vivo*. Autofluorescence, induced by a 337 nm, 700 ps pulsed laser, was split to three wavelength sub-bands using dichroic filters, with each sub-band coupled into a different length of optical fiber for temporal separation. STWRFS allows for fast recording/analysis (few microseconds) of time-resolved fluorescence emission in these sub-bands and rapid scanning. Distinct compositions of excised human atherosclerotic aorta were clearly discriminated over scanning lengths of several centimeters based on fluorescence lifetime and the intensity ratio between 390 and 452 nm. Operation of STWRFS blood flow was further validated in pig femoral arteries *in vivo* using a single-fiber probe integrated with an ultrasound imaging catheter. Current results demonstrate the potential of STWRFS as a tool for real-time optical characterization of arterial tissue composition and for atherosclerosis research and diagnosis.

OCIS codes: (170.6510) Spectroscopy, tissue diagnostics; (300.6500) Spectroscopy, time-resolved.

References and links

1. R. Richards-Kortum, and E. Sevick-Muraca, "Quantitative optical spectroscopy for tissue diagnosis," Annu. Rev. Phys. Chem. **47**(1), 555–606 (1996).
2. J. R. Lakowicz, *Principle of Fluorescence Spectroscopy*, (Springer, 2006).
3. N. Ramanujam, "Fluorescence spectroscopy of neoplastic and non-neoplastic tissues," Neoplasia **2**(1/2), 89–117 (2000).
4. R. A. Schwarz, W. Gao, C. Redden Weber, C. Kurachi, J. J. Lee, A. K. El-Naggar, R. Richards-Kortum, and A. M. Gillenwater, "Noninvasive evaluation of oral lesions using depth-sensitive optical spectroscopy," Cancer **115**(8), 1669–1679 (2009).
5. N. Ramanujam, M. F. Mitchell, A. Mahadevan, S. Warren, S. Thomsen, E. Silva, and R. Richards-Kortum, "In vivo diagnosis of cervical intraepithelial neoplasia using 337-nm-excited laser-induced fluorescence," Proc. Natl. Acad. Sci. U.S.A. **91**(21), 10193–10197 (1994).
6. A. J. Morguet, B. Körber, B. Abel, H. Hippler, V. Wiegand, and H. Kreuzer, "Autofluorescence spectroscopy using a XeCl excimer laser system for simultaneous plaque ablation and fluorescence excitation," Lasers Surg. Med. **14**(3), 238–248 (1994).
7. J. Siegel, D. S. Elson, S. E. Webb, K. C. Lee, A. Vlandas, G. L. Gambaruto, S. Lévêque-Fort, M. J. Lever, P. J. Tadrous, G. W. Stamp, A. L. Wallace, A. Sandison, T. F. Watson, F. Alvarez, and P. M. French, "Studying biological tissue with fluorescence lifetime imaging: microscopy, endoscopy, and complex decay profiles," Appl. Opt. **42**(16), 2995–3004 (2003).

#138865 - $15.00 USD Received 30 Nov 2010; revised 19 Jan 2011; accepted 8 Feb 2011; published 14 Feb 2011

8. O. R. Šćepanović, M. Fitzmaurice, J. A. Gardecki, G. O. Angheloiu, S. Awasthi, J. T. Motz, J. R. Kramer, R. R. Dasari, and M. S. Feld, "Detection of morphological markers of vulnerable atherosclerotic plaque using multimodal spectroscopy," J. Biomed. Opt. **11**(2), 021007 (2006).
9. R. H. Wilson, M. Chandra, J. Scheiman, D. Simeone, B. McKenna, J. Purdy, and M.-A. Mycek, "Optical spectroscopy detects histological hallmarks of pancreatic cancer," Opt. Express **17**(20), 17502–17516 (2009).
10. T. Svensson, J. Swartling, P. Taroni, A. Torricelli, P. Lindblom, C. Ingvar, and S. Andersson-Engels, "Characterization of normal breast tissue heterogeneity using time-resolved near-infrared spectroscopy," Phys. Med. Biol. **50**(11), 2559–2571 (2005).
11. L. Marcu, J. A. Jo, Q. Y. Fang, T. Papaioannou, T. Reil, J. H. Qiao, J. D. Baker, J. A. Freischlag, and M. C. Fishbein, "Detection of rupture-prone atherosclerotic plaques by time-resolved laser-induced fluorescence spectroscopy," Atherosclerosis **204**(1), 156–164 (2009).
12. D. Elson, J. Requejo-Isidro, I. Munro, F. Reavell, J. Siegel, K. Suhling, P. Tadrous, R. Benninger, P. Lanigan, J. McGinty, C. Talbot, B. Treanor, S. Webb, A. Sandison, A. Wallace, D. Davis, J. Lever, M. Neil, D. Phillips, G. Stamp, and P. French, "Time-domain fluorescence lifetime imaging applied to biological tissue," Photochem. Photobiol. Sci. **3**(8), 795–801 (2004).
13. S. Andersson-Engels, G. Canti, R. Cubeddu, C. Eker, C. af Klinteberg, A. Pifferi, K. Svanberg, S. Svanberg, P. Taroni, G. Valentini, and I. Wang, "Preliminary evaluation of two fluorescence imaging methods for the detection and the delineation of basal cell carcinomas of the skin," Lasers Surg. Med. **26**(1), 76–82 (2000).
14. L. Marcu, M. C. Fishbein, J. M. I. Maarek, and W. S. Grundfest, "Discrimination of human coronary artery atherosclerotic lipid-rich lesions by time-resolved laser-induced fluorescence spectroscopy," Arterioscler. Thromb. Vasc. Biol. **21**(7), 1244–1250 (2001).
15. T. J. Pfefer, D. Y. Paithankar, J. M. Poneros, K. T. Schomacker, and N. S. Nishioka, "Temporally and spectrally resolved fluorescence spectroscopy for the detection of high grade dysplasia in Barrett's esophagus," Lasers Surg. Med. **32**(1), 10–16 (2003).
16. J. A. Jo, Q. Fang, T. Papaioannou, J. D. Baker, A. H. Dorafshar, T. Reil, J. H. Qiao, M. C. Fishbein, J. A. Freischlag, and L. Marcu, "Laguerre-based method for analysis of time-resolved fluorescence data: application to in-vivo characterization and diagnosis of atherosclerotic lesions," J. Biomed. Opt. **11**(2), 021004 (2006).
17. Q. Y. Fang, T. Papaioannou, J. A. Jo, R. Vaitha, K. Shastry, and L. Marcu, "Time-domain laser-induced fluorescence spectroscopy apparatus for clinical diagnostics," Rev. Sci. Instrum. **75**(1), 151–162 (2004).
18. Y. Sun, J. Park, D. N. Stephens, J. A. Jo, L. Sun, J. M. Cannata, R. M. G. Saroufeem, K. K. Shung, and L. Marcu, "Development of a dual-modal tissue diagnostic system combining time-resolved fluorescence spectroscopy and ultrasonic backscatter microscopy," Rev. Sci. Instrum. **80**(6), 065104 (2009).
19. Y. Sun, R. Liu, D. S. Elson, C. W. Hollars, J. A. Jo, J. Park, Y. Sun, and L. Marcu, "Simultaneous time- and wavelength-resolved fluorescence spectroscopy for near real-time tissue diagnosis," Opt. Lett. **33**(6), 630–632 (2008).
20. L. Marcu, "Fluorescence lifetime in cardiovascular diagnostics," J. Biomed. Opt. **15**(1), 011106 (2010).
21. D. N. Stephens, J. Park, Y. Sun, T. Papaioannou, and L. Marcu, "Intraluminal fluorescence spectroscopy catheter with ultrasound guidance," J. Biomed. Opt. **14**(3), 030505 (2009).
22. A. J. Lusis, "Atherosclerosis," Nature **407**(6801), 233–241 (2000).
23. J. Sanz, and Z. A. Fayad, "Imaging of atherosclerotic cardiovascular disease," Nature **451**(7181), 953–957 (2008).

1. Introduction

Fluorescence spectroscopy offers great potential for non-invasive disease diagnosis by analyzing the tissue autofluorescence from endogenous fluorophores [1–3]. The detection of cancer and atherosclerosis based on intrinsic fluorescence signals has been widely explored [4–17]. This optical method provides a feasible and quantitative molecular analysis at relatively low cost. Among a number of spectroscopic techniques, time-resolved laser-induced fluorescence spectroscopy (TR-LIFS) is particularly promising for clinical application because this modality not only exhibits a reliable characterization using multiple parameters such as fluorescence intensity, wavelength, and lifetime but is also minimally affected by the irregular tissue surface and the presence of endogenous absorbers [11–17]. Time-resolved fluorescence spectroscopy has developed rapidly in the past two decades and been applied to diagnose tissue diseases including tumors and atherosclerosis [7,11–17]. However, the current application of TR-LIFS is still limited by the time-consuming data acquisition and signal analysis and information extraction [17,18]. To overcome these challenges, we proposed a novel concept for simultaneous time- and wavelength-resolved fluorescence spectroscopy (STWRFS) [19]. This method is able to record fluorescence lifetime at multiple wavelengths sequentially in less than 200 ns using a single detector and light source. Further, wavelength selection is accomplished by inserting specific dichroic filters once the relevant wavelengths are determined for the particular tissue or disease. This design improves the data acquisition speed and reduces the complexity of the instrument.

#138865 - $15.00 USD Received 30 Nov 2010; revised 19 Jan 2011; accepted 8 Feb 2011; published 14 Feb 2011

The TR-LIFS devices tested in medical applications, typically include four key components: a picosecond pulsed laser to induce fluorescence, a monochromator for spectrum scanning, a photomultiplier (picosecond resolution) electronically recording and amplifying the emitted photons, and a fast digitizer (usually an oscilloscope with at least GHz bandwidth) for signal acquisition and analysis [14,15,17,18]. To differentiate fluorophores with overlapping spectra, fluorescence lifetime is used, as particular biomolecules can be identified in complex biological systems based on their temporal decay signature. Both fluorescence lifetime and intensity data are analyzed over a broad spectral range from ultra-violet (UV) up to near infrared. The analysis of these combined data (spectral intensities and lifetimes) provides TR-LIFS with the enhanced capability to detect specific conditions in tissues based on the changes in biochemical composition and metabolism [11,14,16]. However, the application of TR-LIFS in clinical setting is still challenging due to a number of factors including error caused by tissue/patient motion, variation of light intensity affected by blood flow in the optical pathway, and time-consuming measurements at multiple locations due to a single "point" readout. In contrast, a STWRFS system is able to acquire fluorescence lifetime data within multiple spectral bands dynamically while moving across the tissue.

Extending our previously described system, i.e. STWRFS [19], the primary goals of this study were as follows: 1) to optimize and test the STWRFS system for dynamic line scanning of large tissue samples; and 2) to test the STWRFS as a potential tool for dynamic characterization of arterial vessels using intravascular catheters. Based on the STWRFS's fast data acquisition time, this study evaluates the performance of dynamic time-resolved fluorescence measurement while linearly scanning over several centimeters of atherosclerotic tissues samples *ex vivo*, and pig arteries intravascularly under pulsatile blood flow conditions *in vivo*. Secondarily, this study tests STWRFS's ability to work in conjunction with conventional ultrasonic-based tissue diagnostic scanning systems, i.e. ultrasound backscatter microscopy (UBM) and intravascular ultrasound (IVUS). Since the ultrasonic systems provide structural/morphological information about tissues they are complementary to fluorescence-based tissue diagnostic methods such as STWRFS that primarily provide biochemical information. Thus this approach is important for future practical intravascular implementation of STWRFS.

2. Materials and methods

2.1 STWRFS system design and configuration

A schematic of the STWRFS system is illustrated in Fig. 1(a), with a photograph shown in Fig. 1(b). The design consists of a combination of dichroic filters and different lengths of optical fiber. The primary concept of STWRFS was described briefly above and was reported in a previous letter [19], however the optics and electronics in the current system were modified to achieve more efficient fluorescence detection specifically for the lower signal levels found in biological tissue samples. First the laser delivery and fluorescence collection was executed through the same optical fiber, which provided a self-aligned fluorescence excitation and collection probe with a high optical efficiency. This also enabled the design of intravascular catheters in a relatively small diameter. Second, the nitrogen pulsed laser (MNL 205, LTB Lasertechnik Berlin, Germany) used here offered a 16x higher pulse energy (at the fiber output), a 5x higher repetition rate, and a shorter pulse width (40% reduction) compared with the previous system. These parameters not only enabled a higher fluorescence signal but also improved the speed of data acquisition. The compact size of this laser allowed a portable STWRFS on a mobile cart appropriated for in vivo experiments in the animal surgery lab. In addition, the photo-detector and oscilloscope were upgraded to reach a higher temporal resolution as described later. Finally the line scanning function and the incorporation of ultrasound imaging allowed a multi-modal dynamic tissue characterization tool for in vivo application. During STWRFS experiments, tissue autofluorescence was induced using the 337 nm laser with the pulse width of 700 ps and repetition rate up to 50 Hz. The light was delivered (laser excitation) and collected (fluorescence emission) via a single fused silica

#138865 - $15.00 USD Received 30 Nov 2010; revised 19 Jan 2011; accepted 8 Feb 2011; published 14 Feb 2011

optical fiber (NA = 0.22) with a diameter of 400 μm or 600 μm for *in vivo* and *ex vivo* experiments, respectively. The fluorescence was delivered to a series of 45° dichroic filters held in microscope filter cubes (U-MF2, Olympus), and bandpass filters (Semrock, Rochester, NY, USA) so that the light was split into the three sub-bands. The three filters were optimized for the autofluorescence characterization of artery according to our previous work [11,14,16]. They offered higher transmittance (>95%) and more appropriate bandwidths compared with those in previous setup [19]. The first filter (F1: 390/40 nm) corresponded to the peak emission wavelength of collagen and the second filter (F2: 452/45 nm) was designed to record the maximum emission of elastin with a reduced influence from collagen, seen in Fig. 2(b). Filter 3 (F3: 542/50 nm) was chosen to detect the autofluorescence of lipids. The signal was then coupled into three fibers with varying lengths of 1, 10, and 19 m (OZ Optics) using integrated collimation lenses. The proximal ends of the fibers were coupled to a multichannel plate photomultiplier (MCP-PMT, R5916U-50, Hamamatsu, Bridgewater, NJ, USA) which had a rise time of 180 ps. The electronic signals from the MCP-PMT were amplified by a preamplifier (C5594, 1.5G Hz bandwidth, Hamamatsu) and recorded by a digital oscilloscope (DPO7254, 2.5 GHz bandwidth, 20 GHz sampling rate, Tektronix Inc., Richardson, TX, USA). The acquisition was completed in less than 200 ns after one excitation laser pulse. The excitation energy on the sample was set at 2-2.5 μJ to produce sufficient signal but limited photobleaching and phototoxicity. The pulse energy at the fiber output was up to 16 μJ. To improve the signal to noise ratio, fluorescence profiles were averaged over 6-16 samples on the digitizer. The previous STWRFS required the average of 16-256 samples even for fluorescent dye solutions. For intravascular catheter application, a single fiber configuration was design to deliver excitation light and collect fluorescence emission with the same optical fiber. The single fiber function was built in a miniature assembly using a 30 mm cage cube (CW1-4E, Thorlabs, Newton, NJ, USA) containing a dichroic mirror and two SM05 tubes, shown in Fig. 1(a) and 1(b). Inside these tubes, 6 mm quartz lenses were used as beam collimators (f = 10 mm, Thorlabs, Newton, NJ, USA). Optical fibers were mounted on the cage system with SMA adaptors so that it was possible to exchange optical fibers feasibly. The whole system was deigned to be compact and flexible for clinical applications.

2.2 Scanning function and setup

For *ex vivo* tissue scanning experiments a custom-built positioning stage was used to move the optical fiber along the tissue sample surface. This recently reported assembly [18] was originally designed in our lab for bi-modal fluorescence spectroscopy and UBM studies and permits the acquisition of information on both tissue biochemical composition and structural/morphologic data. The positioning system incorporated a precise x-y-z translation stage (MX80L/MX80S, Parker-Daedal, Irwin, PA, USA), a stepper motor (Vix250AH/E-DC, Parker Hannifin, Rohnert Park, CA, USA), and a controller (ACR9000). The maximum travel limit was 50 mm with a positional accuracy of 1 μm. The scanning speed was set at 1 mm/second to accommodate the repetition rate (≤ 50 Hz) of the nitrogen laser. For improved signal to noise ratio, each acquisition averaged the fluorescence from 16 laser pulses. For tissue samples with strong fluorescence emission the average number could be lowered thus enabling faster scanning speeds. For example, for an average of 6 pulses the scanning speed was set at 2 mm/second which resulted in a single line scanning (2 cm distance) in 10 s. During scanning the optical fiber probe was positioned in close proximity to tissue. Due to the irregular tissue surface the probe-to-tissue distance was estimated to vary between 0.5 and 1.5 mm.

2.3 Biomolecules and tissue samples

Collagen type I from bovine Achilles (C9879) and elastin from bovine neck ligament (E1625) were purchased from Sigma. Human aorta samples were obtained post-mortem and frozen within 2 hours of autopsy. They were snap-frozen by first being dipped in isopentane to reduce freezing artifacts and then being dipped in liquid nitrogen and stored at −80°C. The samples were defrosted at 4°C overnight before being spectroscopically investigated. A total

#138865 - $15.00 USD Received 30 Nov 2010; revised 19 Jan 2011; accepted 8 Feb 2011; published 14 Feb 2011

of four aorta samples from three patients were measured using STWRFS. In addition, conventional TR-LIFS measurements of diverse arterial beds similar to those we previously reported [11,14,16,20] were conducted at multiple points along the scanning line of STWRFS. Results were analyzed and compared to verify the new method. Prior to STWRFS measurements, the clinical pathologist identified the regions of interest (plaques of interest) in the excised tissue. This was based on visual inspection. STWRFS linear scanning was performed across these representative areas. The beginning and the end of the scanning line as well as distinct anatomic markers on tissue surface (e.g. protrusions, change in tissue surface color, capillaries, etc) were marked using tissue ink in a specified color code. Then, the tissue was fixed in formalin, pre-cut in a narrow piece (~2 mm thick) along the scanning line, and fixed in paraffin block for pathology analysis. Using a conventional microtome tissue was cut on 4 μm thick sections along the scanning line, mounted on the microscope slides, and stained with conventional H&E and trichrome. All pathology slides were prepared by a qualified technician based on standard protocol. Finally, the pathologist diagnosed the tissue types along the marked site independently without any information from spectroscopy.

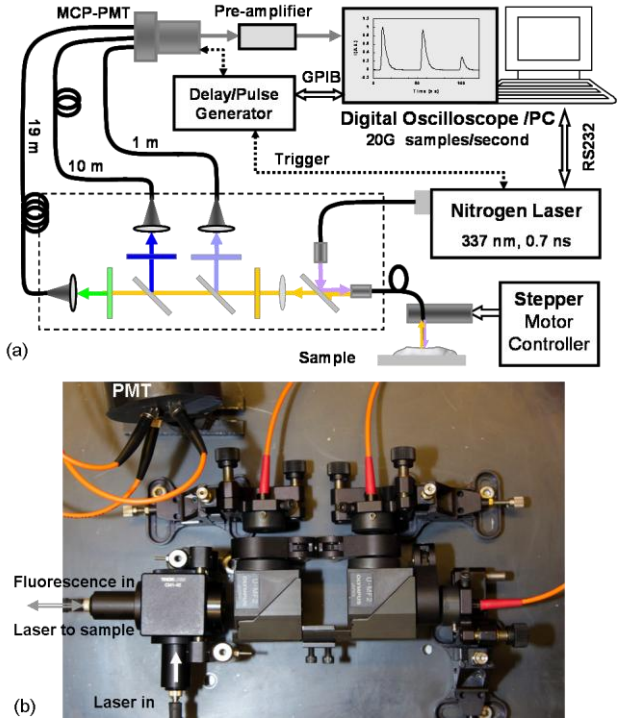

Fig. 1. STWRFS system with a single optical fiber as a probe for excitation delivery and fluorescence collection. (a) System diagram including optical design and electronic configuration. (b) Photograph of the portable optical setup using microscope cubes and micro-lenses.

2.4 In vivo pig experiments

To test the ability of the STWRFS system to operate in an intravascular setting in conjunction with intravascular ultrasound (IVUS) and under blood flow conditions, catheter pullback experiments were performed in healthy arterial wall of three distinct juvenile Yorkshire pigs (40-50 kg) in three independent intravascular application of the catheter that enable for interrogation of 8 arterial segments. Since the fluorescence of such vessel wall is dominated by the emission of elastin fibers in the arterial intima [21], the fluorescence lifetime of these vessels is not expected to have significant variation along a particular arterial wall or from one animal to the other. The experiments were conducted in compliance with and under the

#138865 - $15.00 USD Received 30 Nov 2010; revised 19 Jan 2011; accepted 8 Feb 2011; published 14 Feb 2011

approval of the University of California Institutional Animal Care and Use Committee (IACUC), and the Occupational Health Program at UC Davis. A specialized multi-modality catheter (MMC), similar to a system we previously reported [21], was used for the acquisition of IVUS guided STWRFS. In brief, this includes: a) A commercial 3 Fr IVUS catheter (~1.1 mm diameter, SR Pro 30 MHz, Boston Scientific). b) A customized side-view optical fiber (RoMack, Inc., Williamsburg, VA; 400 μm core, 780 μm outer diameter) was used for STWRFS measurements. This was composed of a multimode fused silica fiber (NA = 0.22) with a 45° polished metalized mirror termination for beam deflection at 90° to the fiber axis. A polyimide tube surrounding the fiber formed a saline flushing channel with the flow rate of 0.07 ml/s for blood removal. The optical fiber can be rotated and positioned independent of the IVUS catheter. c) A guide wire (0.014") that can be used to push (steer) the optical fiber laterally into contact with the artery wall. The tip profile of MMC is less than 2.0 mm in diameter. During experiments pigs were anesthetized and injected with 5000 units of heparin to prevent blood clotting. The right femoral artery was surgically exposed and then the MMC was introduced into a femoral artery through a steerable sheath to an insertion distance of around 20 cm. STWRFS data and IVUS images were recorded simultaneously during experiments.

The fluorescence signals were recorded through all three filters with the PMT gain voltage at around 2 kV and the laser energy at 2.5 μJ/pulse. Two sets of experiments were conducted. (1) The first set represents control experiments or still-mode measurements of the arterial wall fluorescence. In this case, the catheter was placed under IVUS guidance at distinct locations along the artery, pushed in contact with the artery wall and held still for a few tens of seconds to record a group of consecutive data sets (fluorescence decays) in the three channels (Filters 1-3). In this test, the system was adjusted to obtain reliable signals and the instrumental parameters were optimized including laser energy, detector gain, pulse average number, acquisition speed, and saline flushing volumes. (2) The second set was recorded in scanning-mode where the catheter was pulled back along the artery wall and scanned over a distance of a few centimeters. This mimicked a common procedure used by a cardiologist for the examination of the arterial wall during IVUS interventions. The STWRFS measurements were determined at pull-back speeds of 1 mm/s. Each acquisition took 0.5 to 1.0 s when the average number was 6 to 16 pulses/acquisition.

2.5 Software for data acquisition, instrument control, and data processing

A LabVIEW (National Instruments, Austin, Texas) interface was created to control the instrument, conduct data acquisition, and dynamically display the fluorescence intensity, intensity ratio between different emission sub-bands, and fluorescence lifetime. The detailed data analysis, numerical deconvolution of the fluorescence impulse response function (IRF) to remove the system response of the detector and pulsed laser, and calculation of the average lifetime values were conducted after experiments in a graphical user interface programmed in MATLAB (The MathWorks Inc, Natick, MA). In particular, the Laguerre polynomial deconvolution technique was employed to retrieve the fluorescence IRF [16]. This method enabled accurate and rapid lifetime mapping without a priori assumptions of the functional form of the fluorescence decay. The intensity was the integration of the fluorescence pulse profile (the area-under-the-curve of the time-resolved trace). This was equivalent to the steady-sate intensity. In addition, the intensity signals in the three sub-bands were calibrated based on the spectra of standard dyes. This calibration allowed the correction of the transmission of filters and endoscope, and the spectral response of the detector.

3. Results and discussions

3.1 STWRFS system verification on fluorescent biomolecules

Endogenous fluorophores (collagen and elastin) were measured to test the system STWRFS performance and compared with the results obtained with a scanning TR-LIFS system available in the lab previously reported [16]. Fluorescence impulse response profiles were

#138865 - $15.00 USD Received 30 Nov 2010; revised 19 Jan 2011; accepted 8 Feb 2011; published 14 Feb 2011

recorded from collagen and elastin powders at the three wavelength sub-bands as shown in Fig. 2(a). Average lifetimes of collagen were retrieved as 2.94 ± 0.12 and 2.85 ± 0.17 ns after deconvolution for filters F1 and F2, respectively. The signal from filter F3 was too weak for precise lifetime evaluation. Fluorescence lifetimes of elastin for F1, F2, and F3 were 1.72 ± 0.02, 1.81 ± 0.01, and 1.83 ± 0.03 ns, respectively. These values were in good agreement with those reported in the literature [1,17,18].

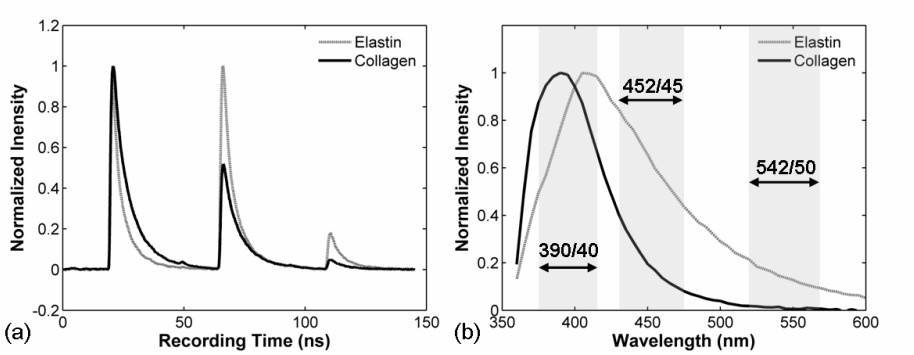

Fig. 2. Measurement of biomolecules elastin and collagen: (a) fluorescence decay profiles and intensity recorded simultaneously at three wavelengths sub-bands (F1, F2, F3) measured within 200 ns. (b) Spectra of the same elastin and collagen samples excited by 337 nm laser measured with a scanning TR-LIFS device [16] and the corresponding sub-bands for F1(390/40), F2(452/45), and F3(542/50) nm filters.

3.2 STWRFS scanning performance – validation on ex-vivo tissue samples

Two representative results from scanning measurements made on *ex vivo* human atherosclerotic aorta using the STWRFS system with the fiber-optic catheter and the motorized stage are summarized in the following.

Figure 3 demonstrates the scanning procedure and results from one sample of atherosclerotic aorta characterized by heterogeneous composition and morphology. During experiments, aorta tissue was opened along the artery axial direction and scanned in the perpendicular direction with a scan length of around 30 mm. The color photograph in Fig. 3(a) shows a human artery tissue with the scanned line used for the measurement marked. This tissue was determined to have three representative regions labeled in the picture as fibrotic plaque, early-stage plaque, and the surrounding normal tissue. This identification was based on visual inspection first and was further tested by histopathology analysis conducted by an independent pathologist according to a trichrome staining. Fibrotic plaque is usually considered to be a late stage lesion that is rich in collagen fibers, while early-stage plaques exhibit developing lipid and collagen accumulation [22,23]. The intensities of the three sub-bands are plotted Fig. 3(c). During the scanning measurements, the fluorescence intensity fluctuated along the tissue surface. Although the intensity in the F1 channel is expected to vary depending on the tissue collagen content, the signal was also affected by the irregular morphology. Thus, the value of the intensity alone was not found reliable for tissue characterization.

Further analysis of intensity ratios for distinct wavelength sub-bands and fluorescence decay characteristics within this sub-bands demonstrated that two sets of parameters show a clear association with tissue types and chemical compositions without being affected by the scanning and irregular morphology. These were the intensity ratio of F1 to F2 (I_{F1}/I_{F2}) and the fluorescence lifetime of F1 (τ_{F1}, 1/e decay time of fluorescence impulse response). Figure 3(d) demonstrates the I_{F1}/I_{F2} and τ_{F1} along the scanning line shown in Fig. 3(a). From left to right this scan traversed a fibrotic plaque, a normal area, and then another fibrotic plaque, which were independently identified based on histopathology analysis. The mean of average lifetimes (τ_{F1}) of the three regions were 2.77 ± 0.18, 1.84 ± 0.08, and 2.33 ± 0.04 ns,

#138865 - $15.00 USD Received 30 Nov 2010; revised 19 Jan 2011; accepted 8 Feb 2011; published 14 Feb 2011

respectively. In addition, the shoulder in this data next to the second peak was consistent with an early-stage plaque (intermediate lesion), with a lifetime of 2.57 ± 0.05 ns. It was found that the fluorescence lifetime increased by 51% for atherosclerotic plaque compared to the surrounding normal tissue. The average intensity ratios (I_{F1}/I_{F2}) in the three regions are 1.26 ± 0.15, 0.67 ± 0.05, and 1.3 ± 0.14, respectively. The intensity ratio rose by 94% in late-stage plaque in contrast to the normal tissue. The early-stage plaque has the intensity ratio at 1.08 ± 0.03. Both I_{F1}/I_{F2} and τ_{F1} allowed clear visualization of the three regions consistent with the tissue types.

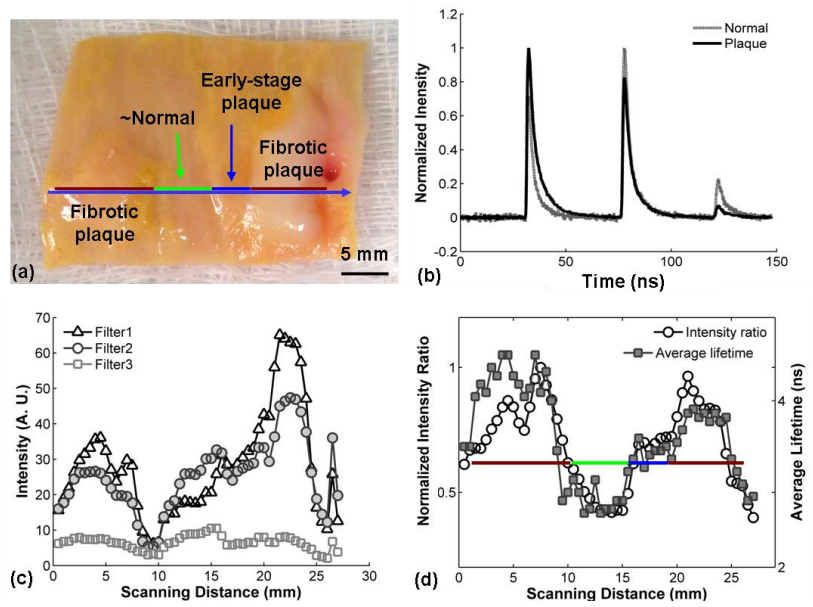

Fig. 3. Example of dynamic scanning of aorta tissue: (a) The aorta was opened and scanned perpendicular to the axial direction. The different regions of tissue were marked with a color bar seen in (a) and (d). (b) STWRFS profiles recorded from a collagen-rich plaque region and the surrounding normal tissue. (c) Fluctuation of the fluorescence intensity along the scanning line from each filter. (d) Variation of fluorescence lifetime and intensity ratios of F1/F2 showing the difference between normal artery and plaque areas. The data shown in (c) and (d) were recorded from a scan measurement crossing the whole tissue from the left to the right shown in (a) with a blue line.

A second scanning measurement of a different human aorta sample is summarized in Fig. 4. This sample included three regions, classified as (from left to right): surrounding normal, early-stage fibrolipidic plaque, and fibrotic plaque with calcified necrotic core, as identified by histopathology results independently from the fluorescence measurement. The three regions were clearly discriminated by I_{F1}/I_{F2} and τ_{F1} as seen in Fig. 4(b). The average lifetimes (τ_{F1}) were also distinctive: 1.88 ± 0.11, 2.37 ± 0.07 and 2.74 ± 0.08 ns, respectively. Here the lifetime increased 46% for fibrotic plaque compared with the normal tissue. The average intensity ratio (I_{F1}/I_{F2}) also increased in the three regions from 0.75 ± 0.08, to 1.44 ± 0.08, and then to 1.55 ± 0.32 respectively. The intensity ratio rose over 107% in the third stage. These trends are in agreement with our earlier publication [11,14,16,20] reporting on the time-resolved fluorescence characteristics of arterial beds including atherosclerotic aorta.

This second aorta sample was also used to demonstrate the corroboration of fluorescence data with the UBM image (obtained with an unfocused single element 45 MHz transducer) used to visualize the tissue structural features (axial and lateral resolutions 38 and 200 μm, respectively) in the cross section under the scanned line, as shown in Fig. 4(c). The image shows the thickened intimal layer at the top of the tissue cross section that corresponds to the

#138865 - $15.00 USD Received 30 Nov 2010; revised 19 Jan 2011; accepted 8 Feb 2011; published 14 Feb 2011

early stage and fibrotic plaques areas. The region corresponding to the advanced fibrotic plaque also exhibited an increased hyperechoic region in the top layers corresponding to the dense collagen structure and ultrasound reflection (acoustic shadow) indicating the presence of a calcified necrotic core underneath the fibrotic cap. These features were also validated by histopathological analysis of the sample.

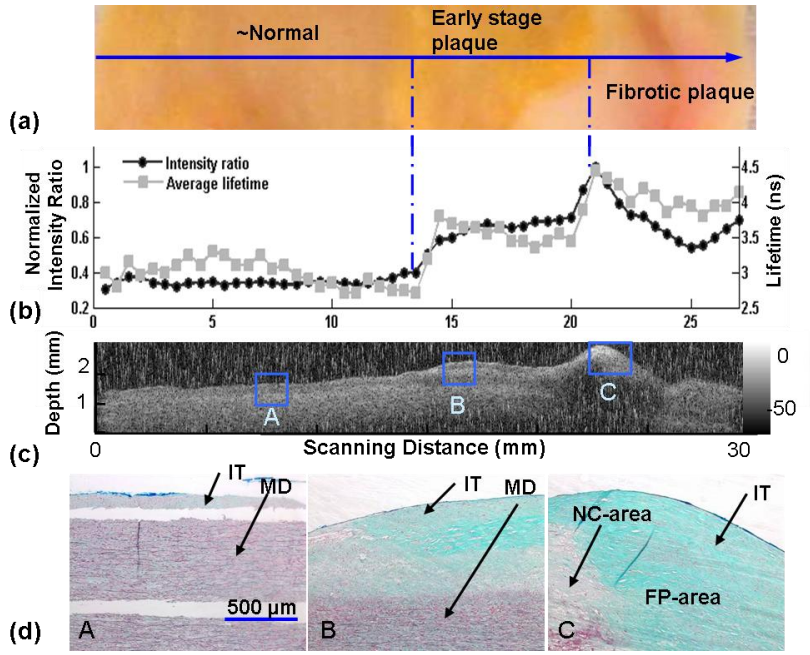

Fig. 4. Comparison of STWRFS results with pathology analysis and ultrasound imaging: (a) Close-up photograph of the tissue scanned through three regions: surrounding normal, early-stage plaque, and fibrotic plaque. The arrow indicates the scanning direction. (b) Fluorescence lifetime and intensity ratio show differentiation of three regions (scan time ~10 sec). (c) Ultrasound image of the cross section of the artery showing structural feature of the plaque. (d) Histopathology results (thricrome staining) used to confirmed the classification of normal (A-area), early-stage lipidic plaque (B-area), and fibrotic plaque (C-area) consistent with our interpretation of the STWRFS measurement. IT – intima layer; MD – media layer; LP – lipid rich area within thickened intima; FP – collagen rich area within intima; NC – necrotic area within intima.

Figure 4(d) displays the representative images of three types of tissue from trichrome staining histopathology slides used to validate the STWRFS and UBM measurements: A - normal, B - early-stage plaque with intracellular lipid accumulation collagen fiber formation, C - fibrotic plaque with lipid core and fibrotic/calcific regions. Trichrome staining is a common method for differentiating structural proteins (collagen, elastin fibers), smooth muscle cells, and to distinguish these from the other lipidic and calcified structures in plaques. It can be observed that the main component in normal tissue (A-area) is elastin as depicted by the dark coloration lines in the media of the healthy aorta. Within the 250 μm arterial penetration depth estimated at 337 nm [12], the thickened intima of early stage plaque (B-area) contain a combination of collagen (green) and lipid-rich areas including macrophages and lipid components (white areas). In fibrotic plaque (C-area) the whole cross section is rich in collagen fibers. Part of a large necrotic cores is also visible on the button left of the tissue histology section.

The fluorescence results are seen to be consistent with tissue composition because both intensity ratios and fluorescence lifetimes vary depending on the ratio of collagen (F1) to elastin (F2). The elastin was the main endogenous fluorophore in healthy artery wall while the composition of collagen gradually increased with the progression of atherosclerosis

#138865 - $15.00 USD Received 30 Nov 2010; revised 19 Jan 2011; accepted 8 Feb 2011; published 14 Feb 2011

[11,22,23]. Plaque tissue with more collagen showed a higher $I_{F1/F2}$ value compared with the normal artery. Furthermore, τ_{F1} was dominated by the collagen lifetime component (2.5 to 5 ns), which was found longer than that of elastin (~1.5 ns). Therefore, the plaque showed a relatively long lifetime compared with normal tissue. The shorter fluorescence lifetime of early stage plaque (rich in collagen and lipids) relative to fibrotic plaques (primarily rich in collagen) denotes the contribution of short-lived fluorescent lipid components (~1 ns) to the overall fluorescence decay dynamics.

3.3 STWRFS scanning performance – validation in vivo

The scanning (catheter pullback sequence) experiments conducted intravascularly *in vivo* in swine arteries under IVUS guidance were used to evaluate the ability of the STWRFS apparatus to record robust fluorescence lifetime data in conditions that mimic conventional catheterization procedures including IVUS. The *in vivo* intravascular STWRFS application faced several challenges including the limitation on the diameter of optical probe, attenuation of fluorescence intensity by blood absorption, operation of the catheter in pulsatile blood flow, and the constraint for a rapid dynamic measurement. Therefore the requirement for light collection efficiency and probe positioning were much stricter than other types of application on open tissue surfaces.

Representative results from the still-mode (control) measurements are displayed in Fig. 5(a), 5(b), and 5(c) showing the intensity, intensity ratio, and average lifetime at different times. Each data set was recorded over a one second time interval at the same location. The fluorescence intensity showed weak variation between different pulses but the intensity ratio and lifetime were found to be constant, as shown in Fig. 5 (a), 5(b) and 5(c). The intensity ratios of I_{F1}/I_{F2}, I_{F1}/I_{F3}, and I_{F2}/I_{F3} were 0.42 ± 0.01, 1.49 ± 0.02, 3.57 ± 0.05, respectively. The average fluorescence lifetimes were 1.60 ± 0.01 ns and 1.86 ± 0.05 ns for F1 and F2, respectively. Due to the low intensity values with F3 it was difficult to achieve a robust deconvolution of the fluorescence IRF, thus lifetime values for F3 are not presented.

Here both florescence intensity ratio and lifetime values were in a good agreement with fluorescence of the pig normal arterial wall that is rich in elastin [21]. Blood absorption had previously been investigated since it was a major concern in the optical design for the illumination and fluorescence collection. 337 nm light has very limited penetration depth in blood, which also has strong absorption at the fluorescence wavelengths under investigation. It is possible for these factors to cause the loss or distortion of autofluorescence signal of artery when measured *in vivo* in pulsatile blood flow. We determined that in still-mode all spectroscopic variables investigated here (intensities ratios and lifetimes) remained constant during the measurement. These results suggest that when the catheter is in contact with tissue the blood flow in the artery did not have an obvious effect on the autofluorescence measurement. It also indicates that the MMC catheter and STWRFS provide robust results at a very low flushing rate of 0.07-0.1 ml/s.

Representative results from the scanning-mode experiments are depicted in Fig. 5(d), 5(e), and 5(f) for intensity, intensity ratio, and average lifetime at different positions along the artery wall. It was observed that the fluorescence intensity fluctuated significantly when the catheter moved along the lumen (Fig. 5(d)). This effect is most likely a result of (1) changes in light excitation-emission geometry due to fluctuations of the distance between the probe and sidewall and changes in the lumen diameter; and (2) attenuation of light intensity due to diffusion of blood between fiber optic tip and arterial wall. Although more robust when compared to intensity values, the intensity ratio values for the three filters also fluctuated especially for I_{F1}/I_{F3} (Fig. 5(e)). Findings suggest that a ratiometric intensity measurement does not fully compensate for factors that affect the fluorescence intensity. The average intensity ratios of I_{F1}/I_{F2}, I_{F1}/I_{F3}, and I_{F2}/I_{F3} are 0.49 ± 0.02, 1.76 ± 0.08, 3.58 ± 0.05, respectively.

#138865 - $15.00 USD Received 30 Nov 2010; revised 19 Jan 2011; accepted 8 Feb 2011; published 14 Feb 2011

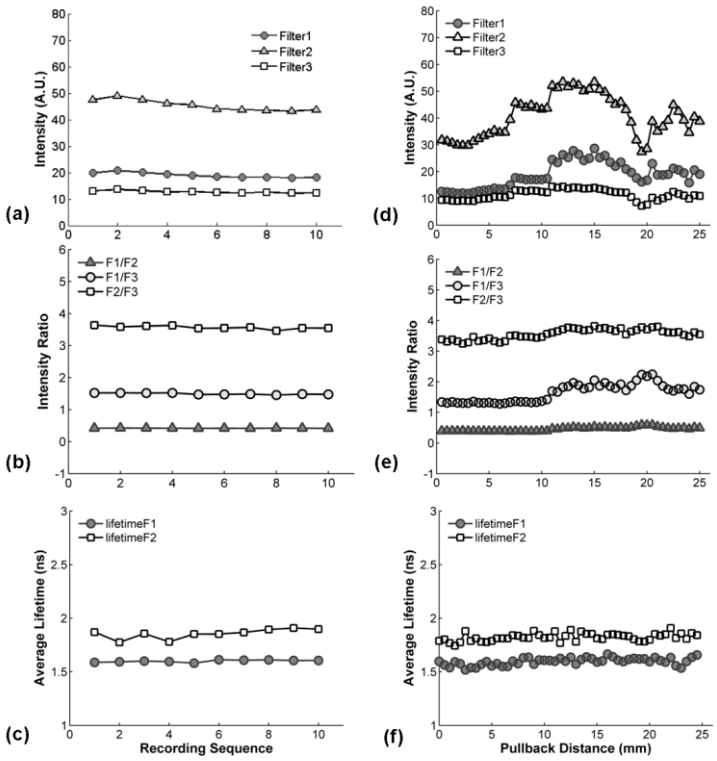

Fig. 5. In vivo test of STWRFS in pig femoral artery: (a), (b), and (c) are the data in still mode – the probe was held at the same location (~1 second) for multiple measurements. (d), (e), and (f) are the results from a pull-back measurement when the catheter was gently moved along the axial direction for 25 mm. (a) and (d) show fluorescence intensity for the three filters, (b) and (e) display the intensity ratios, and (c) and (f) show the lifetimes.

The fluorescence lifetimes values for F1 and F2 were constant during pullback measurements (Fig. 5(f)) with values of 1.60 ± 0.03 ns and 1.82 ± 0.04 ns, respectively. The constant fluorescence lifetime indicated the composition of the artery wall along the lumen is similar, which was consistent with our expectation because the fluorescence of healthy young pig artery is primarily due to elastin emission as previously shown and confirmed by histology. Similar average fluorescence lifetime results depicting small standard deviation values (<0.05 ns) or intra-animal variability were obtained for each of the eight arterial segments linearly scanned in vivo. Moreover, the average fluorescence value (mean ± SD) for all independent measurements (total of 8 arterial segments) conducted in vivo in all animals was determined as 1.70 ± 0.16 for F1 and 1.8 ± 0.06 for F2. The larger SD value in this latter case is due to inter-animal mean lifetime value variability rather than intra-animal mean lifetime value changes. These findings also indicated that the MMC catheter and STWRFS when deployed in the close proximity of the vessel wall and pulled back provide robust results at a very low flushing rate of 0.07-0.1 ml/s during dynamic fluorescence recording.

4. Conclusions

This work has applied STWRFS to dynamic tissue characterization in the study of arterial vessel fluorescence *ex vivo* and *in vivo*. The near real-time acquisition of time-resolved fluorescence spectra has been approached based on the simultaneous measurement of multiple emissions split spatially by bandpass filters and synchronized temporally with optical fibers. Using this technique, the autofluorescence of large-scale specimens of human artery were scanned and studied to differentiate atherosclerotic plaque regions from surrounding normal tissue. It was found that the fluorescence intensity ratio and fluorescence lifetime at distinct

#138865 - $15.00 USD Received 30 Nov 2010; revised 19 Jan 2011; accepted 8 Feb 2011; published 14 Feb 2011

spectral bands (e.g. ratio of 390 nm / 452 nm; lifetime at 390 nm) were both associated with the presence of atherosclerotic lesions. For example, the fluorescence lifetime increased over 46% in the regions of fibrotic plaque compared with the surrounding normal tissue. The changes in chemical composition of tissue were reflected in these two parameters and were consistent with pathological results. Also, these parameters appeared independent of changes in sample illumination geometry during scanning such as the tissue surface relief due to the presence of plaque.

Furthermore, STWRFS has been successfully validated for the first time *in vivo* for the intravascular examination on a pull back sequence using a prototype multi-modal catheter combining a single-fiber optical probe, a conventional IVUS catheter, a steering wire enabling contact or close proximity between the fiber probe and arterial vessel, and a saline flushing channel for blood removal in the optical field of view. The two test modes (still and scanning) showed that STWRFS was able to record reliable autofluorescence signals from a healthy pig femoral artery in both modes. Most importantly, while the intensity measurements showed large fluctuations due to range of factors that affect the light intensity (e.g, illumination geometry, blood vessel cross-section geometry, and blood absorption), the fluorescence lifetime values provided a reliable way for the characterization of tissue composition independent of these light intensity modulating factors.

Overall, both *in vivo* and *ex vivo* measurements demonstrate that STWRFS technique provides robust fluorescence lifetime data concerning the composition of the arterial wall under dynamic (scanning) measurement conditions. In addition, we showed that STWRFS can be intraluminaly applied and guided using conventional catheterization procedures and IVUS catheters. Moreover, experiments conducted in atherosclerotic tissue samples using the combined STWRFS and UBM system demonstrate that a combination of fluorescence and ultrasonic data enable simultaneous recording of biochemical and structural features, respectively. Future experiments are planned to determine the ability of the integrated STWRFS and IVUS systems to diagnose atherosclerotic plaques intravascularly in an atherosclerotic animal model.

Acknowledgements

This work was supported in part by the National Institutes of Health (Grants R01-HL67377, R21-EB003628, and UL1 RR024146), the NSF Center for Biophotonics Science and Technology, and the Cancer Center at UC Davis. The authors would like to thank Dr. William T. Ferrier and Linda Talken for their technical help on animal experiments.

#138865 - $15.00 USD Received 30 Nov 2010; revised 19 Jan 2011; accepted 8 Feb 2011; published 14 Feb 2011